Anal Bioanal Chem (2013) 405:6479–6487
DOI 10.1007/s00216-013-7080-1

RESEARCH PAPER

Molecularly imprinted polymers as synthetic receptors for the QCM-D-based detection of L-nicotine in diluted saliva and urine samples

J. Alenus · A. Ethirajan · F. Horemans · A. Weustenraed · P. Csipai · J. Gruber · M. Peeters · T. J. Cleij · P. Wagner

Received: 19 February 2013 / Revised: 26 April 2013 / Accepted: 21 May 2013 / Published online: 11 June 2013

Abstract Molecularly imprinted polymers (MIPs) are synthetic receptors that are able to specifically bind their target molecules in complex samples, making them a versatile tool in biosensor technology. The combination of MIPs as a recognition element with quartz crystal microbalances (QCM-D with dissipation monitoring) gives a straightforward and sensitive device, which can simultaneously measure frequency and dissipation changes. In this work, bulk-polymerized L-nicotine MIPs were used to test the feasibility of L-nicotine detection in saliva and urine samples. First, L-nicotine-spiked saliva and urine were measured after dilution in demineralized water and 0.1× phosphate-buffered saline solution for proof-of-concept purposes. L-nicotine could indeed be detected specifically in the biologically relevant micromolar concentration range. After successfully testing on spiked samples, saliva was analyzed, which was collected during chewing of either nicotine tablets with different concentrations or of smokeless tobacco. The MIPs in combination with QCM-D were able to distinguish clearly between these samples: This proves the functioning of the concept with saliva, which mediates the oral uptake of nicotine as an alternative to the consumption of cigarettes.

Keywords Molecularly imprinted polymers · L-nicotine · Nicotine tablets · Smokeless tobacco · Quartz crystal microbalance · Dissipation monitoring

This paper is dedicated to Professor Franz Dickert on the occasion of his 70th birthday.

J. Alenus · A. Ethirajan · F. Horemans · A. Weustenraed · P. Csipai · M. Peeters · T. J. Cleij · P. Wagner
Institute for Materials Research (IMO),
Hasselt University, Wetenschapspark 1,
3590 Diepenbeek, Belgium

P. Csipai · J. Gruber
Instituto de Química, Universidade de São Paulo,
Av. Prof. Lineu Prestes, 748,
CEP 05508-000 São Paulo, SP, Brazil

M. Peeters · P. Wagner (✉)
Division IMOMEC, IMEC, Wetenschapspark 1,
3590 Diepenbeek, Belgium
e-mail: Patrick.Wagner@uhasselt.be

Introduction

Molecularly imprinted polymers (MIPs) are synthetic receptors that can capture low molecular weight molecules in a selective manner [1–4]. This makes them a candidate for use in biomimetic sensing technology [5–7]. Compared to conventional recognition elements, such as antibodies and enzymes, they are easily and cheaply produced in large quantities and have a long shelf life as they do not degrade under ambient circumstances [8, 9]. These characteristics make them ideal for applications in a variety of scientific fields like environmental analysis [10], food analysis [11, 12], separation technology [13, 14], and biosensing [15]. In biosensing applications, detection of the binding event using MIPs can be achieved with electrochemical transducers based on membranes [16], piezoelectric [17], and optical transducers [18]. Targets for MIP detection can be low molecular weight molecules [8, 19, 20], proteins [21, 22], DNA [23], and whole cells [24]. During synthesis, first a pre-polymerization complex is formed between template and functional monomers. Then, the preformed complex is polymerized and fixed by the aid of cross-linker monomers.

After polymerization, the template molecule is extracted, thereby leaving tailor-made cavities behind which can selectively rebind the template molecule. The effectiveness of MIPs in biosensor technology has already been demonstrated in aqueous media like demineralized water (dH_2O) and phosphate-buffered saline solution (PBS) [25, 26]. The next step is to verify the usefulness of MIPs in biosensor technology by detecting the desired molecule in "real-life" matrices such as human blood serum [27, 28], urine [27], saliva [29], blood plasma [20], natural waters, and soil samples [10]. In this work, a MIP was created for the detection of L-nicotine in aqueous media including urine and saliva.

L-nicotine is the major addictive substance found in tobacco and is usually taken up in the human body through smoking, chewing, or sniffing tobacco. In the framework of nicotine replacement therapies for smoking cessation, nicotine can be administered using gums and tablets, nicotine patches, inhalers, and nasal sprays [30–32]. This raises the question on the most efficient way of nicotine delivery keeping in mind that in case of oral intake (gums and tablets), a large fraction of the nicotine is swallowed and will not enter the bloodstream. A first quantification of this lost fraction can be achieved by determining the amount of nicotine present in saliva. Tobacco smoke, until now the most common pathway of nicotine intake, contains besides L-nicotine more than 4,000 compounds of which more than 50 are carcinogenic [33]. It has been proven that tobacco consumption causes a higher risk for the development of cancer in the lungs and respiratory tract [34, 35] and diseases such as pulmonary disease [36], atherosclerosis [37], and periodontal disease [38]. The presence of L-nicotine can be determined in various samples such as urine, hair, breast milk, plasma, and saliva [39]. The detection of L-nicotine is preferably done in a noninvasive way with easily obtained samples. Saliva is simply collected from test persons and, shortly after consumption of products containing L-nicotine, the concentration of L-nicotine is higher than the cotinine concentration [40]. It is important to measure the L-nicotine concentrations in their natural matrix as this will give the most accurate result. Detection in saliva has been established with several methods such as liquid-phase microextraction and high-performance liquid chromatography coupled with UV–vis detection [39]. The analysis of L-nicotine and its oxidation products in nicotine chewing gum has been reported with molecularly imprinted solid-phase extraction, but these tests were not yet performed in saliva [29]. The detection techniques used so far are complex, time consuming, and require trained personal, which makes them disadvantageous. Quartz crystal microbalance-dissipation (QCM-D) provides a fast, easy, and reliable testing platform for the use of MIPs in combination with body fluids. MIPs are immobilized on the quartz crystal via a polyvinyl chloride (PVC) adhesion layer. When L-nicotine binds to the MIP, the resonance frequency of the quartz crystals will shift according to the added mass as described by the Sauerbrey equation [41]. Binding of the template can also cause shifts in the dissipation of the functionalized quartz crystal: This is measured after every excitation and is an indication for the loss of vibrational energy. These changes are due to conformational and viscoelastic changes at the surface and can serve also as an additional read-out technique [42, 43]. In a previous work, the binding capacities of the MIP were already studied in L-nicotine-spiked dH_2O and PBS using the QCM-D setup, showing specific binding of the target in both fluids [43]. In this contribution, the MIPs' efficiency to bind L-nicotine in more complex fluids was tested with saliva and urine samples. As a start, the saliva and urine samples were spiked with L-nicotine and subsequently diluted with dH_2O or PBS. For further validation of the sensor, a test person was instructed to chew nicotine chewing gums with a concentration of 2 or 4 mg L-nicotine to obtain saliva samples with different concentrations. As a second trial, a test person was instructed to consume smokeless tobacco. These saliva samples were tested with the MIP sensor to investigate whether the L-nicotine can be detected in these matrices. The various tests demonstrate the practicality, specificity, and sensitivity of the MIP-based QCM-D sensor platform for these analytical tasks.

Materials and methods

Reagents

The molecularly imprinted polymer was synthesized using ethylene glycol dimethacrylate (EGDM) as the cross-linker, methacrylic acid (MAA) as functional monomer, and hexane as the porogen. Prior to polymerization, the stabilizers in the MAA and EGDM were removed by passing through an alumina column. For the initiator, azobisisobutyronitrile (AIBN) was used. All chemicals employed in the polymerization were of analytical grade and obtained from various commercial sources. The PVC adhesive was purchased from

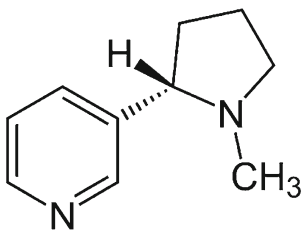

Fig. 1 Structure of L-nicotine

Sigma-Aldrich NV/SA, Bornem, Belgium. The target molecule L-nicotine, $C_{10}H_{14}N_2$ (MW, 162.23 Da; see Fig. 1 for the chemical structure), was obtained from Acros Organics, Geel, Belgium. The nicotine chewing gums (Nicorette®, Johnson & Johnson NV, Beerse, Belgium) were used in concentrations of 2 and 4 mg L-nicotine per tablet while nicotine-free "taste samples" of the Nicorette® gums were employed for reference purposes. The smokeless tobacco was Skoal® Wintergreen Longcut, Stamford, CT, USA.

Equipment

The morphology of the sensor surface was studied by optical microscopy with a Zeiss Axiovert 40 MAT (Carl Zeiss, Jena, Germany). Microscope images were processed using the image analysis program ImageJ 1.37v from the National Institute of Health, Bethesda, USA. Quartz crystals (5 MHz) with Cr/Au electrodes were purchased from LOT-Oriel (Darmstadt, Germany). The QCM system (Q-sense E4) was also purchased from LOT-Oriel (manufacturer Q-Sense, Gothenburg, Sweden). A flow setup was established with a peristaltic pump (IPC-N) from Ismatec.

MIP synthesis

For the preparation of the L-nicotine MIP, a mixture of MAA (12.5 mmol), EGDM (25.5 mmol), and AIBN (0.66 mmol) was dissolved in 7 ml hexane together with the template molecule L-nicotine (6.41 mmol). To exclude oxygen in the mixture, it was degassed for 10 min with N_2. Subsequently for polymerization, the solution was sealed and kept in a thermostatic water bath at 60 °C (72 h). After polymerization, the solid MIP was ground with a mechanical mortar (24 h) and passed through a 25-μm sieve. Only particles with a size smaller than 25 μm were used. Next, the L-nicotine was extracted from the MIP powder by extensive washing with methanol (48 h), followed by a mixture of acetic acid/acetonitrile (1/1) (48 h) and finally again with methanol (12 h) using a continuous extraction setup. A non-imprinted polymer (NIP) was synthesized as a reference material in the same way but without the presence of the target molecule.

Sensing system

The QCM crystals have a resonance frequency of 5 MHz and are modified with Cr/Au electrodes. The Q-Sense E4 system allows for simultaneous measurements of up to four crystals. The system is temperature controlled and was kept at 22.00±0.01 °C throughout the measurements. On the top electrode, a layer of PVC (PVC 0.35 wt% in tetrahydrofuran) was spin coated (5,000 rpm with 990 rpm/s) to obtain a layer of 100-nm thickness. The MIP was then applied onto the surface using a poly(dimethylsiloxane) stamp, which was pressed against the active sensing surface. This resulted in a thin layer of MIPs on the surface. Subsequently, the PVC was heated to 120 °C for 15 min. As this temperature is well above the glass transition temperature of 80 °C, the MIP particles partially sink into the polymer layer. The samples were then cooled and the excessive MIP powder was rinsed off with deionized water. QCM measurements were performed as follows: First, the system was left to stabilize in the fluid (dH_2O or 0.1× PBS at pH 9) in which the performance of the MIP was to be tested. This was at a flow rate of 200 μl/min. After the signal was stable, L-nicotine-spiked saliva or urine samples were diluted with the measuring fluid (dH_2O or PBS) to achieve various concentrations that were then consecutively connected to the flow system starting with the lowest concentration while keeping the flow rate constant. In between the exposures to the different concentrations, the sensor was flushed with dH_2O in order to ensure the recovery to the sensor baseline before testing the next higher concentration. This results in a dose–response curve for the frequency and dissipation of the QCM-D system. The frequency noise was 0±0.84 Hz on average while the noise on the dissipation signal was $0\pm0.43\times10^{-6}$ on average. All measurements were performed six times per concentration in dH_2O or 0.1× PBS at pH 9. In the "Results and discussion" section, the average response per concentration is presented while the error bars correspond to the standard deviation.

Sample preparation

In Fig. 2, the sample preparation protocol is schematically presented. In order to collect saliva, a nonsmoker test person was asked to deposit saliva in a sterilized Falcon tube every minute until the desired amount of 40 ml was met. This saliva was immediately centrifuged for 10 min with 10,000 rpm at 8 °C (a). The supernatant was collected (b) and filtered using 1 μm syringe filters (c). This resulting saliva sample was split in two parts. One part of the collected saliva was spiked with L-nicotine (100 mM) (d) while the other half was unaltered (e) serving as a control fluid. The same procedure was used on urine samples. Fluids were stored at −18 °C to prevent degradation. For measurement purposes, the L-nicotine-spiked saliva and urine samples were diluted from the stock solution to the desired concentrations using dH_2O or PBS. These are indicated as "spiked with L-nicotine" in the resulting graphs. For example, a nicotine concentration of 100 μM was obtained by diluting 20 μl of the 100 mM stock solution (volume measured with a micropipette, precision <0.5 μl) with dH_2O or PBS to a final volume of 20 ml. The non-spiked saliva and urine sample volumes used are the same as the volumes of the L-nicotine-spiked samples used to create the corresponding concentration. These are indicated as "without L-nicotine" in the resulting graphs.

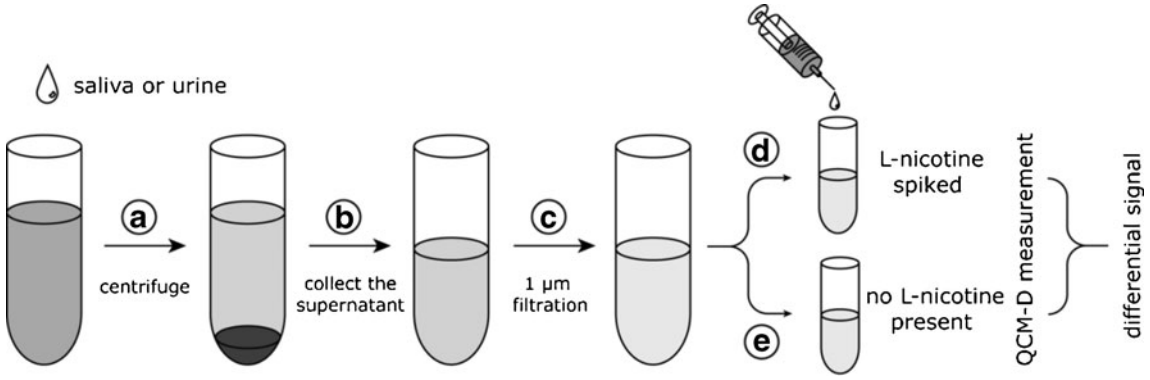

Fig. 2 Sample preparation. The collected nonsmoker saliva or urine sample is first centrifuged at 10,000 rpm for 10 min (**a**) and then the supernatant is collected (**b**) and filtered (**c**). One half is spiked with L-nicotine (**d**) while the other half is not altered (**e**)

Results and discussion

An average surface coverage of the QCM crystals was 19.4 % for the MIP and 20.2 % for the NIP powders, which is consistent with previously reported surface coverage values [26]. All shown QCM-D results (except for the raw data in Fig. 3a) are differential data where the nonspecific NIP response was subtracted from the MIP response. The NIP channel serves as a control and will show the nonspecific binding, while the MIP represents the specific binding of L-nicotine on top of nonspecific events. By subtracting the NIP from the MIP response, the specific binding of the L-nicotine is obtained, which gives a direct insight in the performance of the sensor.

L-nicotine detection in saliva

The saliva was collected according to the "Sample presentation" section. One part was spiked with L-nicotine (100 mM) and subsequently diluted with dH_2O or 0.1× PBS of pH 9 to obtain the required concentrations. The other part remained unaltered and served as a control. The results of these measurements are shown in Fig. 3.

As can be seen in Fig. 3a, the MIP and NIP gave no significant frequency response with non-spiked saliva of a nonsmoking test person. This means that there is little tendency to bind other molecules than L-nicotine in saliva. With spiked saliva, the frequency drop for the MIP is significantly stronger than for the NIP, indicating specific binding of the L-nicotine. Figure 3b shows the MIP–NIP difference signal between spiked- and non-spiked saliva. With the spiked saliva, the frequency drops in a sublinear way with increasing concentration. A spiked concentration of 20 µM L-nicotine results in a frequency shift of 10±4 Hz, while a spiked concentration of 100 µM L-nicotine causes a 37±5-Hz frequency drop. To give an estimate for the limit of detection (LOD) and the limit of quantification (LOQ), we consider the initial, linear slope, which is −0.48 Hz/µM. The uncertainty of the frequency measurement is 1.7 Hz (two times the frequency noise of ±0.84 Hz) and the LOD (three times the uncertainty) will therefore correspond to 10.6 µM while the LOQ (five times the uncertainty) is 17.7 µM. The saliva sample without L-nicotine does not show a frequency drop and stays stable, suggesting that nonspecific binding to MIP and to NIP is comparable and weak. This means that the MIP is able to recognize and bind the L-nicotine present in the spiked saliva in a specific manner. While measuring the frequency change, the QCM-D simultaneously measures changes in the dissipation. The same experiment was also performed with saliva diluted in 0.1× PBS at pH 9, as PBS mimics the ionic composition of body liquids. The pH of 9 was used on purpose because earlier studies suggested that the employed MIP has an optimal binding capacity for L-nicotine at this pH value [43]. From Fig. 3c, it is clear that the sensitivity of the MIP decreases significantly in comparison to measurements in dH_2O. A concentration of 100 µM of L-nicotine results in a 15±4-Hz frequency drop in 0.1× PBS at pH 9 while in dH_20, the frequency drop is 37±5 Hz. On average, the MIP is able to bind almost three times more L-nicotine from the same spiked saliva sample when measured in dH_2O than in 0.1× PBS at pH 9. The lowered binding capacity of the MIP in 0.1× PBS at pH 9 may be attributed to interfering ions in the electrolyte, which hinder the formation of hydrogen bridges between the MIPs and the L-nicotine molecules.

In Fig. 4, the change in dissipation is shown for saliva-spiked and non-spiked samples, which were diluted in dH_2O. It is apparent that only the L-nicotine-spiked saliva samples resulted in changes in dissipation, again confirming that the MIP is able to bind L-nicotine specifically. The difference between the L-nicotine-spiked sample and the non-spiked sample is less pronounced than the frequency

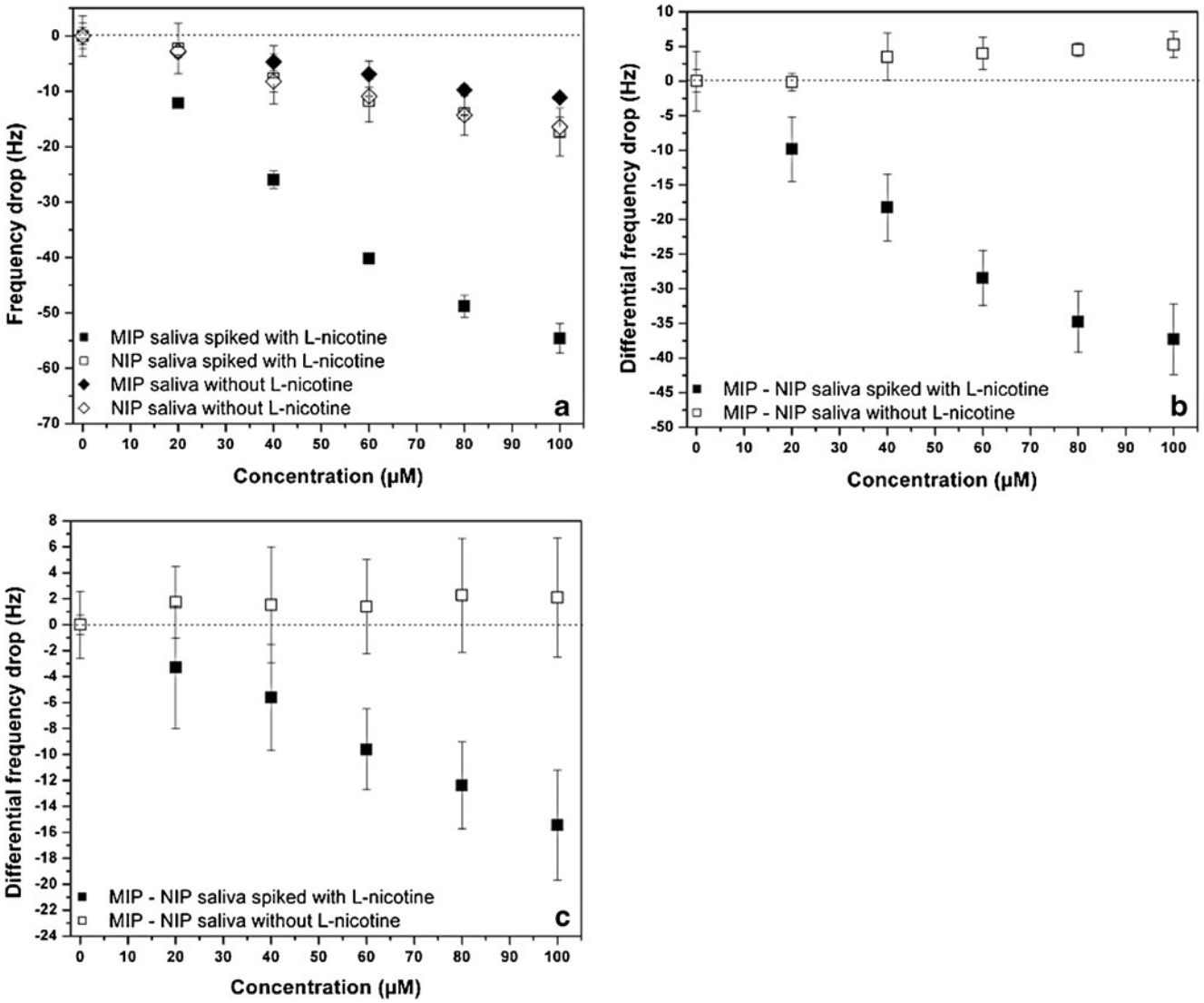

Fig. 3 (**a**) Dose–response curve for the saliva samples spiked with L-nicotine: the spiked saliva was diluted with dH_2O to obtain the required concentrations. Data for the MIP are given as *solid squares* while the NIP data are presented by *open squares*. The same measurements, however with non-spiked saliva, are presented as *solid diamonds* (MIP) and *open diamonds* (NIP). (**b**) Differential MIP–NIP signal for spiked (*solid squares*) and non-spiked saliva samples (*open squares*), diluted in dH_2O. (**c**) Differential MIP–NIP signal when the spiked (*solid squares*) and non-spiked saliva samples (*open squares*) were diluted in 0.1× PBS of pH 9

changes documented in Fig. 3b, but nevertheless, a distinction can be made between the two. This proves that also dissipation measurements can serve for the detection of low molecular weight molecules in diluted body fluids. The dissipation is determined by the viscoelastic properties of the interface between the quartz crystal and the liquid under study. We point out that the increasing nicotine concentration goes along with a larger portion of saliva diluted in dH_2O, leading by itself to a higher dissipation. However, the differential measurement shown in Fig. 4 corrects for this viscoelastic response, proving that the recognition of nicotine alters the viscoelastic behavior of the MIP layer itself. To our knowledge, this observation has not been reported in prior literature.

L-nicotine detection in urine

To further prove the ability of MIPs to bind L-nicotine specifically in complex matrices, the same tests were performed in urine. Urine was chosen because in smokers' urine, there are still traces of L-nicotine present. Also, urine is a complex matrix with a composition distinctly different from saliva. We mention that most of the L-nicotine is metabolized in the body to cotinine, which is excreted through urine [44]. The MIP and NIP were previously tested for cross selectivity towards cotinine, which did indeed not show significant binding [43]. Although the other molecules present in urine differ strongly from the ones present in saliva, the results obtained with urine samples are similar

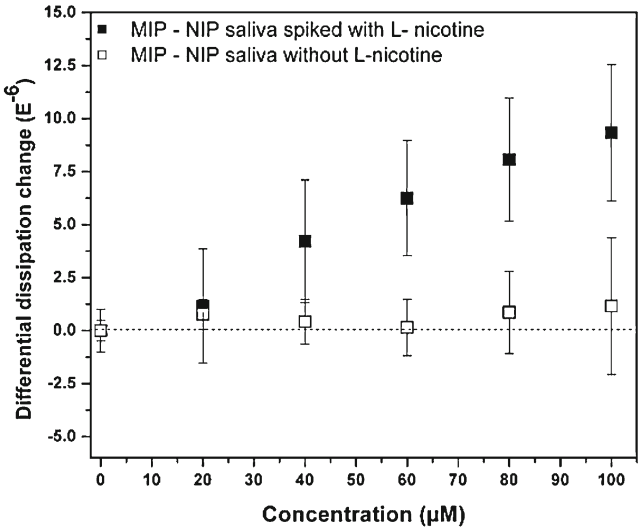

Fig. 4 Differential MIP–NIP dose–response curve of the dissipation signal for increasing concentrations of spiked L-nicotine saliva (*solid squares*) and non-spiked saliva (*open squares*). All measurements were performed on spiked and non-spiked saliva samples diluted in dH_2O

to the ones obtained with saliva. In Fig. 5, the differential signal for the L-nicotine-spiked urine and non-spiked urine is presented. A concentration of 10 µM L-nicotine results in a frequency shift of 31±1 Hz, while a concentration of 100 µM L-nicotine causes a 54±2-Hz frequency drop. It should be noted that the signal seems to saturate at a concentration of 60 µM. The L-nicotine-spiked samples cause a stronger frequency change than the non-spiked urine sample indicating that L-nicotine is specifically bound to MIPs from the urine matrix. This proves that the MIP can specifically detect L-nicotine in at least two different diluted body fluids.

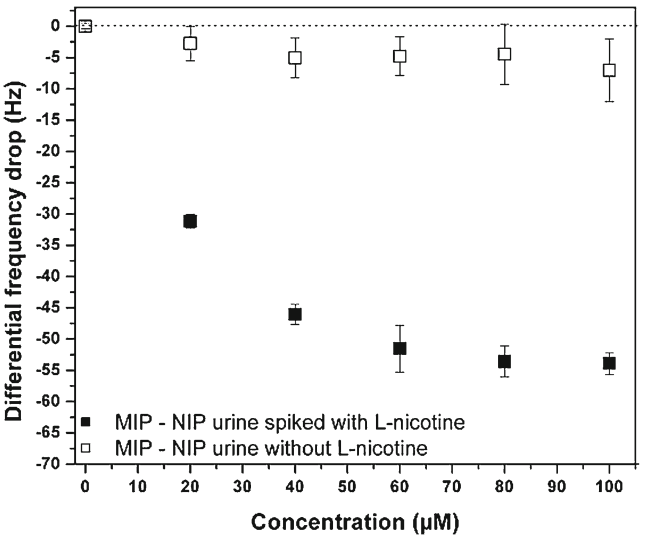

Fig. 5 Differential MIP–NIP dose–response curves for urine samples spiked with L-nicotine (*solid squares*) and non-spiked urine samples (*open squares*). The spiked- and non-spiked urine samples were diluted in dH_2O to obtain the indicated concentrations

Detection of L-nicotine from saliva collected while chewing nicotine gums and smokeless tobacco

As a confirmation test for the selective and specific binding of L-nicotine from a complex matrix, the MIP sensor was applied to saliva samples collected while chewing nicotine gums with 2 mg and with 4 mg L-nicotine per tablet. The nicotine-free taste samples of the Nicorette® gums were used for reference purposes, allowing correcting for a theoretical, nonspecific sensor response due to flavorings, colorants, and other additives. The test person chewed the nicotine gums for 60 min, meanwhile collecting saliva in a sterilized Falcon tube. Prior to collecting saliva, the test person had no intake of nicotine in any form for at least 24 h in order to avoid possible offset effects. Additionally, saliva samples were obtained during the consumption of 2 g of smokeless tobacco (Skoal® Wintergreen) with a nominal nicotine content of 10 mg L-nicotine per gram as determined in prior literature [45]. Saliva collection, centrifugation, filtration, and storage were handled in the same way as for all other saliva and urine samples (see Fig. 2, except for the spiking in step D).

Figure 6 shows the differential frequency response (response of the MIP-loaded QCM minus the response of NIP-loaded QCM crystals) for the saliva samples obtained with 0, 2, and 4 mg Nicorette® tablets. For all experiments, 0.25 ml of saliva was diluted in 19.75 ml dH_2O to a total sample volume of 20 ml. Due to this strong dilution, we do not expect adverse effects on the resonance frequency, which would be expected due to the viscosity of non-diluted saliva. Differential sensing is a necessity allowing to correct for nonspecific adsorption effects inherent to the

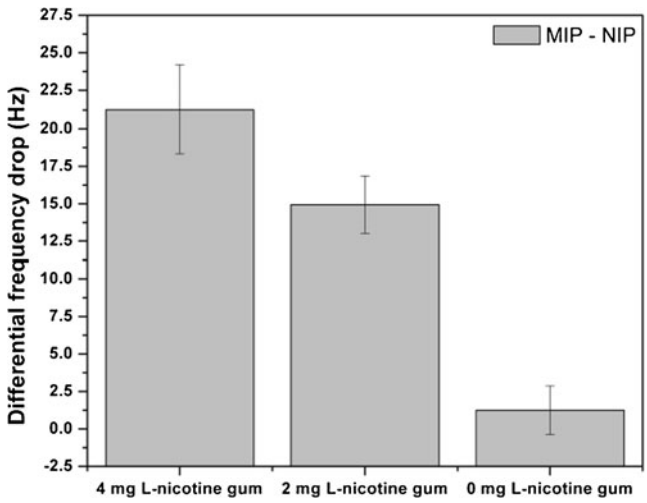

Fig. 6 Differential frequency response of the QCM-D for saliva samples collected while chewing 4 mg nicotine gum, 2 mg nicotine gum, and the nicotine-free (0 mg) taste sample. All data are averaged over six independent measurements. The sensor response of the taste sample is negligible as compared to the error bar

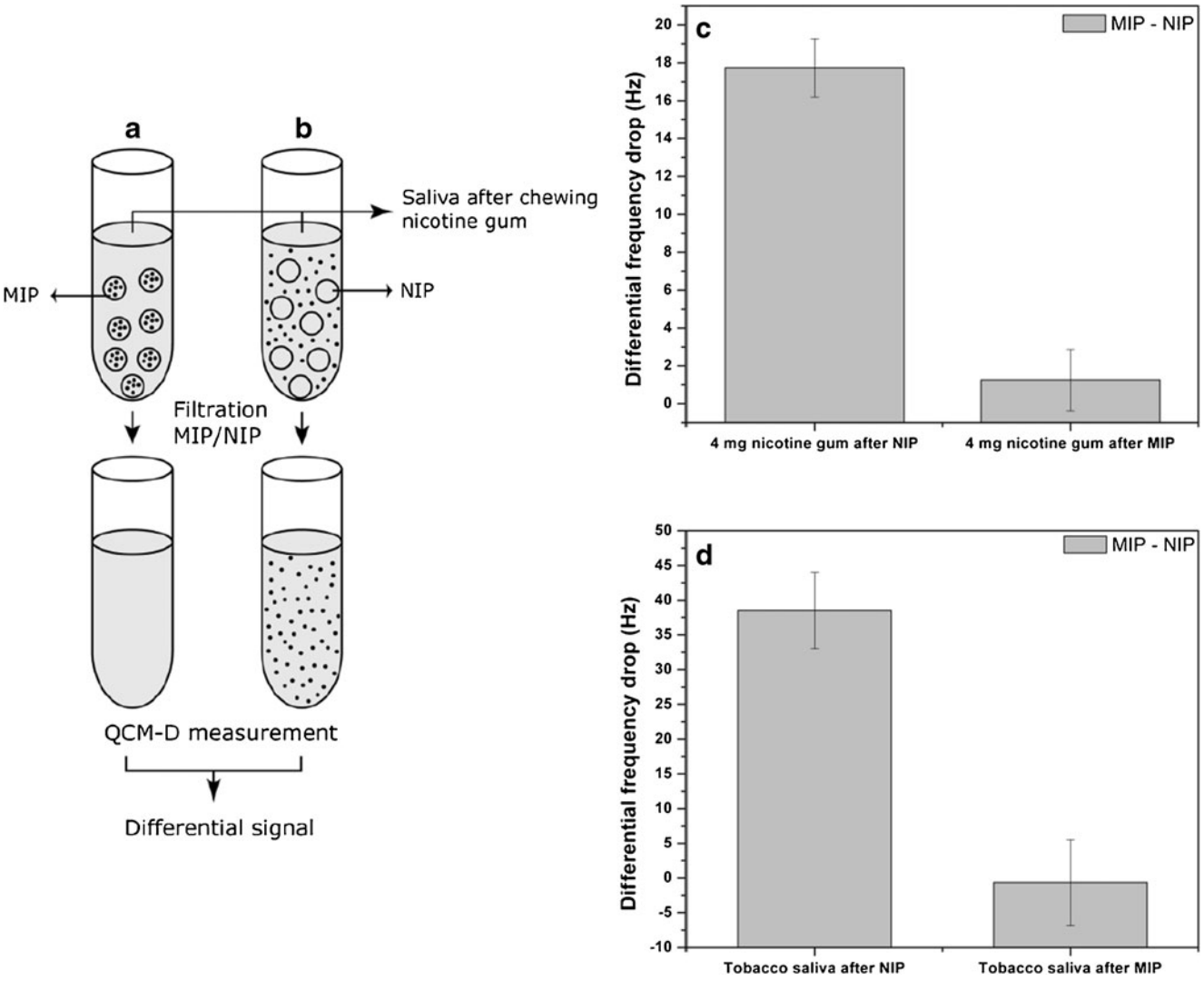

Fig. 7 QCM-D measurements on saliva samples obtained with 4 mg nicotine tablets and with smokeless tobacco. Each sample was either extracted with MIP powder (**a**) or with NIP powder (**b**) with negligible nicotine absorption. (**c**) Differential sensor response for NIP- or MIP-extracted samples obtained with a 4-mg nicotine tablet. The results for NIP- and MIP-extracted saliva obtained while consuming smokeless tobacco are shown in (**d**)

complex mixture of proteins and enzymes in saliva and additives of the Nicorette® tablets. All measurements were performed six times and averaged while the error bars represent the scattering of the data. As expected, the strongest signal change is found with the 4-mg samples (21±3 Hz). It is weaker for the samples obtained with 2 mg tablets (14.5± 1.5 Hz), and with the nicotine-free testing tablet, we measured a signal change of 1±1 Hz. Within the experimental resolution, this corresponds to the complete absence of a recognition effect. Note that the 4-mg samples do not result in twice the response observed with the 2-mg tablets because consuming tablets with higher nicotine concentration stimulates a stronger release of saliva, resulting in dilution. In the sense of the dose–response curve shown in Fig. 3b, the frequency drop of 21 Hz observed with the 4-mg tablet would correspond to a concentration in the range of 43.8±6.2 μM. Assuming that all nicotine from the tablet (4 mg, molecular weight 162.23 g/mol) is transferred to saliva (volume of 8.5 ml after centrifugation and filtering), we expect a nicotine concentration of 2.9 mM in the actual saliva sample. Keeping in mind that these samples were diluted 80 times (0.25 ml of saliva in 19.75 ml dH_2O), we end up with a final concentration of about 36 μM. Within the error bars, this is in reasonable agreement with the value of 44 μM determined from the dose–response curve. In order to confirm the result obtained with QCM with a second, independent technique, we analyzed the same saliva sample with impedance spectroscopy and obtained 43.5± 4.4 μM (using the same degree of dilution). The underlying methodology and calibration curves can be found in reference [46], and this indicates that impedance spectroscopy can be considered as an alternative to the QCM approach described within this article.

Finally, we evaluated whether it is possible to define a sensor baseline in case that neither nicotine-free tablets nor nicotine-free saliva is available as reference materials. For these experiments, two 5-ml samples of diluted saliva (dilution as described above) from the "4-mg nicotine batch" were extracted using either 20 mg of MIP powder or 20 mg of NIP powder. This procedure is schematically illustrated in Fig. 7a, b. The extraction treatment was performed for 120 min at room temperature on a rocking table followed by filtering and collecting the supernatant. In addition to the extraction of proteins and enzymes, which is already achieved by the NIP powder, the MIP powder will also extract the nicotine present in the diluted saliva sample. It is shown in Fig. 7c that the NIP extraction has only a minor influence on the sensor response when compared to the non-extracted samples in Fig. 6. On the other hand, Fig. 7c demonstrates that extraction with MIP powder removes all nicotine and, within error bars, the differential signal remains indeed at the baseline.

The differential sensor response with the NIP-extracted smokeless tobacco sample corresponds to 39±5 Hz, being more than twice as strong as the response obtained with the 4-mg nicotine gum samples. This is in principle not surprising because the nominal total nicotine content of 2 g of smokeless tobacco is not less than 20 mg. In the sense of the dose–response curve in Fig. 3b, the frequency drop by 40 Hz is equivalent to a concentration in the range of about 100 μM. Here, we point out that this concentration is only indicative because smokeless tobacco contains not only flavorings but also salts and pH agents, which stimulate the actual nicotine uptake via the mucous tissue in the oral cavity. Nevertheless, the experiments indicate that there must be a massive release of nicotine, exceeding the response obtained with tablets that are usually employed to reduce the withdrawal symptoms of former smokers.

Conclusion

A MIP with a high affinity and specificity towards L-nicotine has been developed for the use in aqueous fluids. This MIP was successfully integrated in a QCM-D sensor crystal by immobilizing them into a spin-coated PVC layer on top of the upper gold electrode. The MIP performance to specifically bind L-nicotine in biological solutions was tested with spiked saliva and urine samples diluted into dH_2O or 0.1× PBS. First, the MIP was tested with dH_2O where it showed a sublinear frequency response to increasing L-nicotine concentration in the lower micromolar range while the control samples showed no specific response. Dissipation response results were also promising and may serve as an alternative way to differentiate between nicotine-spiked and non-spiked saliva samples. The same experiment was also performed in 0.1× PBS at pH 9 with L-nicotine-spiked saliva samples. The frequency response was lower in comparison with dH_2O, but L-nicotine could still be successfully detected in the micromolar range. The use of the MIP sensor in patients' samples was tested with saliva obtained during chewing of nicotine gums with different standard concentrations and while using smokeless tobacco. The sensor was indeed able to distinguish between different concentrations of L-nicotine in saliva while chewing nicotine gums. Consistently, we observed a strong nicotine release when consuming smokeless tobacco. This illustrates that MIPs are versatile receptors for small-molecule detection in complex fluids when combined with quartz crystal microbalances or other analytical techniques used in the pharmaceutical, environmental, and bioanalytical sectors.

Acknowledgments This work is supported by an IMEC Ph.D. Fellowship (J. Alenus), by the Life-Science Initiative of the Province of Limburg (M. Peeters), and by the Internationalization Program of Universidade de São Paulo, Brazil (P. Csipai). The authors also would like to thank H. Penxten, J. Soogen, C. Willems, and J. Baccus cordially for technical assistance.

References

1. Cormack PA, Elorza AZ (2004) Molecularly imprinted polymers: synthesis and characterisation. J Chromatogr B 804:173–182
2. Batra D, Shea KJ (2003) Combinatorial methods in molecular imprinting. Curr Opin Chem Biol 3:434–442
3. Sellergren B (2000) Imprinted polymers with memory for small molecules, proteins, or crystals. Angew Chem Int Ed 6:1031–1037
4. Mayes AG, Whitcombe MJ (2005) Synthetic strategies for the generation of molecularly imprinted organic polymers. Adv Drug Deliv Rev 12:1742–1778
5. Dong J, Gao N, Peng Y, Guo C, Lv Z, Wang Y et al (2012) Surface plasmon resonance sensor for profenofos detection using molecularly imprinted thin film as recognition element. Food Control 2:543–549
6. Wei C, Zhou H, Zhou J (2011) Ultrasensitively sensing acephate using molecular imprinting techniques on a surface plasmon resonance sensor. Talanta 5:1422–1427
7. Tsuru N, Kikuchi M, Kawaguchi H, Shiratori S (2006) A quartz crystal microbalance sensor coated with MIP for "Bisphenol A" and its properties. Thin Solid Films 1–2:380–385
8. Horemans F, Alenus J, Bongaers E, Weustenraed A, Thoelen R, Duchateau J et al (2010) MIP-based sensor platforms for the detection of histamine in the nano- and micromolar range in aqueous media. Sensors Actuators B Chem 2:392–398
9. Piletsky SA, Alcock S, Turner AP (2001) Molecular imprinting: at the edge of the third millennium. Trends Biotechnol 1:9–12
10. Alizadeh T, Zare M, Ganjali MR, Norouzi P, Tavana B (2010) A new molecularly imprinted polymer (MIP)-based electrochemical sensor for monitoring 2,4,6-trinitrotoluene (TNT) in natural waters and soil samples. Biosens Bioelectron 5:1166–1172
11. Sun H, Mo ZH, Choy JTS, Zhu DR, Fung YS (2008) Piezoelectric quartz crystal sensor for sensing taste-causing compounds in food. Sensors Actuators B Chemical 1:148–158
12. Jiang X, Zhao C, Jiang N, Zhang H, Liu M (2008) Selective solid-phase extraction using molecular imprinted polymer for the analysis of diethylstilbestrol. Food Chem 3:1061–1067

13. Bereczki A, Tolokán A, Horvai G, Horváth V, Lanza F, Hall AJ et al (2001) Determination of phenytoin in plasma by molecularly imprinted solid-phase extraction. J Chromatogr A 1–2:31–38
14. Masqué N, Marcé R, Borrull F (2001) Molecularly imprinted polymers: new tailor-made materials for selective solid-phase extraction. TrAC Trends Anal Chem 9:477–486
15. Ansell RJ, Kriz D, Mosbach K (1996) Molecularly imprinted polymers for bioanalysis: chromatography, binding assays and biomimetic sensors. Curr Opin Biotechnol 1:89–94
16. Huang J, Xing X, Zhang X, He X, Lin Q, Lian W et al (2011) A molecularly imprinted electrochemical sensor based on multiwalled carbon nanotube-gold nanoparticle composites and chitosan for the detection of tyramine. Food Res Int 1:276–281
17. Lin TY, Hu CH, Chou TC (2004) Determination of albumin concentration by MIP-QCM sensor. Biosens Bioelectron 1:75–81
18. Valero-Navarro A, Salinas-Castillo A, Fernández-Sánchez JF, Segura-Carretero A, Mallavia R, Fernández-Gutiérrez A (2009) The development of a MIP-optosensor for the detection of monoamine naphthalenes in drinking water. Biosens Bioelectron 7:2305–2311
19. Haupt K, Mosbach K (1998) Plastic antibodies: developments and applications. Trends Biotechnol 11:468–475
20. Peeters M, Troost FJ, van Grinsven B, Horemans F, Alenus J, Murib MS et al (2012) MIP-based biomimetic sensor for the electronic detection of serotonin in human blood plasma. Sensors Actuators B Chem 17:602–610
21. Shi H, Tsai W-B, Garrison MD, Ferrari S, Ratner BD (1999) Template-imprinted nanostructured surfaces for protein recognition. Nature 6728:593–597
22. Lu C-H, Zhang Y, Tang S-F, Fang Z-B, Yang H-H, Chen X et al (2012) Sensing HIV related protein using epitope imprinted hydrophilic polymer coated quartz crystal microbalance. Biosens Bioelectron 31(1):439–444
23. Ogiso M, Minoura N, Shinbo T, Shimizu T (2007) DNA detection system using molecularly imprinted polymer as the gel matrix in electrophoresis. Biosens Bioelectron 9–10:1974–1981
24. Hayden O, Bindeus R, Haderspöck C, Mann KJ, Wirl B, Dickert FL (2003) Mass-sensitive detection of cells, viruses and enzymes with artificial receptors. Sensors Actuators B Chem 1–3:316–319
25. Bongaers E, Alenus J, Horemans F, Weustenraed A, Lutsen L, Vanderzande D et al (2010) A MIP–based biomimetic sensor for the impedimetric detection of histamine in different pH environments. Phys Status Solidi A 4:837–843
26. Thoelen R, Vansweevelt R, Duchateau J, Horemans F, D'Haen J, Lutsen L et al (2008) A MIP-based impedimetric sensor for the detection of low-MW molecules. Biosens Bioelectron 6:913–918
27. Patel AK, Sharma PS, Prasad BB (2010) Trace-level sensing of creatine in real sample using a zwitterionic molecularly imprinted polymer brush grafted to sol–gel modified graphite electrode. Thin Solid Films 10:2847–2853
28. Prasad BB, Srivastava S, Tiwari K, Sharma PS (2009) Trace-level sensing of dopamine in real samples using molecularly imprinted polymer-sensor. Biochem Eng J 2–3:232–239
29. Zander A, Findlay P, Renner T, Sellergren B, Swietlow A (1998) Analysis of nicotine and its oxidation products in nicotine chewing gum by a molecularly imprinted solid phase extraction. Anal Chem 15:3304–3314
30. Neal LB (1997) The role of nicotine in smoking-related cardiovascular disease. Prev Med 4:412–417
31. Stead LF, Perera R, Mant D, Lancaster T (2008) Nicotine replacement therapy for smoking cessation (review). Cochrane Database of Systematic Reviews 1: article number CD000146
32. Beard E, Michie S, Fidler J, West R (2013) Use of nicotine replacement therapy in situations involving temporary abstinence from smoking: a national survey of English smokers. Addict Behav 38:1876–1879
33. Hoffmann D, Djordjevic MV, Hoffmann I (1997) The changing cigarette. Prev Med 4:427–434
34. Schrek R, Baker LA, Ballard GP, Dolgoff S (1950) Tobacco smoking as an etiologic factor in disease. I. Cancer. Cancer Res 1:49–58
35. Doll R, Peto R (1981) The causes of cancer: quantitative estimates of avoidable risks of cancer in the United States today. J Natl Cancer Inst 6:1191
36. Mayer AS, Newman LS (2001) Genetic and environmental modulation of chronic obstructive pulmonary disease. Respir Physiol 1:3–11
37. Ambrose JA, Barua RS (2004) The pathophysiology of cigarette smoking and cardiovascular disease: an update. J Am Coll Cardiol 10:1731–1737
38. Bergström J (2004) Tobacco smoking and chronic destructive periodontal disease. Odontology 1:1–8
39. Yang XL, Luo MB, Ding JH (2007) Rapid determination of nicotine in saliva by liquid phase microextraction-high performance liquid chromatography. Chin J Anal Chem 2:171–174
40. Robson N, Bond AJ, Wolff K (2012) Salivary nicotine and cotinine concentrations in unstimulated and stimulated saliva. SSRN eLibrary. Afr J Pharm Pharacol 4(2):061–065. Available from: http://papers.ssrn.com/sol3/papers.cfm?abstract_id=2024696. Accessed Feb 2010
41. Sauerbrey G (1959) Verwendung von Schwingquarzen zur Wägung dünner Schichten und zur Mikrowägung. Z Phys A Hadrons Nuclei 2:206–222
42. Reimhult K, Yoshimatsu K, Risveden K, Chen S, Ye L, Krozer A (2008) Characterization of QCM sensor surfaces coated with molecularly imprinted nanoparticles. Biosens Bioelectron 12:1908–1914
43. Alenus J, Galar P, Ethirajan A, Horemans F, Weustenraed A, Cleij TJ et al (2012) Detection of L–nicotine with dissipation mode quartz crystal microbalance using molecular imprinted polymers. Phys Status Solidi A 5:905–910
44. Behera D, Uppal R, Majumdar S (2003) Urinary levels of nicotine & cotinine in tobacco users. Indian J Med Res 118:129–133
45. Henningfield JE, Radzius A, Cone EJ (1995) Estimation of available nicotine content of six smokeless tobacco products. Tob Control 1:57–61
46. Peeters M, Csipai P, Geerets B, Weustenraed A, van Grinsven B, Gruber J, et al (2013) Heat-transfer based detection of L-nicotine, histamine, and serotonin using molecularly imprinted polymers as biomimetic receptors. Analytical and Bioanalytical Chemistry. doi:10.1007/s00216-013-7024-9